AAC
Journals.ASM.org

Immunoadjuvant Chemotherapy of Visceral Leishmaniasis in Hamsters Using Amphotericin B-Encapsulated Nanoemulsion Template-Based Chitosan Nanocapsules

Shalini Asthana,[a] Anil K. Jaiswal,[b] Pramod K. Gupta,[a] Vivek K. Pawar,[a] Anuradha Dube,[b] Manish K. Chourasia[a]

Pharmaceutics Division, CSIR—Central Drug Research Institute, Lucknow, Uttar Pradesh, India[a]; Parasitology Division, CSIR—Central Drug Research Institute, Lucknow, Uttar Pradesh, India[b]

The accessible treatment options for life-threatening neglected visceral leishmaniasis (VL) disease have problems with efficacy, stability, adverse effects, and cost, making treatment a complex issue. Here we formulated nanometric amphotericin B (AmB)-encapsulated chitosan nanocapsules (CNC-AmB) using a polymer deposition technique mediated by nanoemulsion template fabrication. CNC-AmB exhibited good steric stability *in vitro*, where the chitosan content was found to be efficient at preventing destabilization in the presence of protein and Ca^{2+}. A toxicity study on the model cell line J774A and erythrocytes revealed that CNC-AmB was less toxic than commercialized AmB formulations such as Fungizone and AmBisome. The results of *in vitro* (macrophage-amastigote system; 50% inhibitory concentration [IC_{50}], 0.19 ± 0.04 μg AmB/ml) and *in vivo* (*Leishmania donovani*-infected hamsters; 86.1% ± 2.08% parasite inhibition) experiments in conjunction with effective internalization by macrophages illustrated the efficacy of CNC-AmB at augmenting antileishmanial properties. Quantitative mRNA analysis by real-time PCR (RT-PCR) showed that the improved effect was synergized with the upregulation of tumor necrosis factor alpha (TNF-α), interleukin-12 (IL-12), and inducible nitric oxide synthase and with the downregulation of transforming growth factor β (TGF-β), IL-10, and IL-4. These research findings suggest that a cost-effective CNC-AmB immunoadjuvant chemotherapeutic delivery system could be a viable alternative to the current high-cost commercial lipid-based formulations.

Visceral leishmaniasis (VL), a vector-borne disease, is caused by intramacrophage trypanosomatid protozoa of the genus *Leishmania* (1, 2). VL is manifested by hematological and hepatosplenic abnormalities with defective T-cell-dependent immune responses and is usually fatal if not treated properly (3, 4). Human VL causes an estimated 50,000 deaths annually, a rate surpassed among parasitic diseases only by malaria, and 2,357,000 disability-adjusted life years lost, placing leishmaniasis ninth in a global analysis of infectious diseases (5).

Despite the availability of several chemotherapeutic drugs, successful management of VL has not yet been attained. Indeed, amphotericin B (AmB) is used as a prototype leishmanicidal drug due to its excellent efficacy, with great commercial success. It possesses selective killing activity against *Leishmania* parasites, mediated through its higher binding affinity for 24-substituted sterols (ergosterol and episterol) predominant in the plasma membranes of parasites, since these sterols are not found in mammalian cells (6). However, toxic side effects, in particular hematological intolerance and nephrotoxicity, produced by AmB at therapeutic doses have often limited its clinical application (7).

In the past few years, the capability of drug delivery systems has been critically tested to enhance the accessibility of the drug to reticuloendothelial system (RES) organs (the liver and spleen), ensuring the delivery of smaller amounts to the kidneys and lungs, and thus decreasing AmB-mediated toxicity (8, 9). The investigations of such newer, less-toxic formulations of AmB have led to the development of commercial preparations for therapeutic use such as liposomal AmBisome; Abelcet, an AmB-lipid complex; and micellar Amphotec (10, 11). Although liposomes and lipid complexes have succeeded in reducing the adverse effects of AmB, their lower stability and prohibitively high cost restrict their clinical utility. In contrast, a mixed micellar formulation is cost-effective but cannot improve the tolerability of AmB. Accordingly, there is a need for the development of stable and tolerable low-cost formulations.

We therefore developed novel stable nanoemulsion template (NET)-based polymeric chitosan nanocapsule (CNC) formulations of AmB that have an oil-based central cavity, which represents hydrophobic lipid particles, while the surrounding chitosan has hydrophilic properties. The amphiphilic properties are produced by the inclusion of an oil phase in an oppositely charged chitosan polymer (see Fig. S1 in the supplemental material). The resulting nanocapsule carrier loads easily and can be used to stabilize a greater amount of insoluble hydrophobic or amphiphilic drugs. The rationale behind the choice of chitosan biopolymer includes its excellent biocompatibility, biodegradability (12), and "generally regarded as safe" (GRAS) approval (13) and its cell-mediated immune-enhancing effects, favoring elevated uptake of the carrier system by macrophages (MPϕ) (14). Stimulation of Th1 and suppression of Th2 immune responses are considered a promising therapeutic strategy for leishmaniasis (15), and chitosan has been reported to stimulate MPϕ to produce various

Received 29 September 2012 **Returned for modification** 21 November 2012
Accepted 18 January 2013
Published ahead of print 28 January 2013
Address correspondence to Manish K. Chourasia, manish_chourasia@cdri.res.in.
This article is CDRI communication 8384.
Supplemental material for this article may be found at http://dx.doi.org/AAC.01984-12.

doi:10.1128/AAC.01984-12

proinflammatory cytokines, including interleukin 1 (IL-1), IL-6, tumor necrosis factor alpha (TNF-α), nitric oxide (NO), and granulocyte-MPϕ colony-stimulating factor (GM-CSF) (14, 16, 17). Chitosan also induces immunologic adjuvant effects by active binding to the specific receptors on MPϕ (18–20). Furthermore, the acid-resistive property of chitosan in overcoming immediate lysosomal digestion within MPϕ for a short duration is another advantage favorable to provide sustained AmB release at the particular target site (RES organs, host for the intramacrophage *Leishmania* parasite). Additionally, the ability of chitosan to adsorb to lipid droplets (21), resulting in long-term physically stable polymeric CNCs in both liquid and dry forms, makes these CNCs uniquely applicable as a substitute for the much less stable liposomes.

In the present paper, we report the design and evaluation for antileishmanial efficacy of an AmB carrier system (CNC-AmB) developed for *Leishmania donovani* amastigotes, tested in an experimental model of visceral leishmaniasis in hamsters as well as in a murine macrophage cell line (J774A). The activity of CNC-AmB was compared with those of the commercially available Fungizone and AmBisome formulations. Moreover, the immunomodulatory role of nanocarriers was assessed in hamsters, and a cytotoxicity study was carried out with J774A cells and erythrocytes.

MATERIALS AND METHODS

Materials. AmB was a kind gift from Intas Pharmaceuticals (Ahmedabad, India). Soya lecithin, soya bean oil, Tween 80, low-molecular-weight (LMW) chitosan (deacetylation, 75 to 85%; viscosity, 20 to 200 cP), and MTT (3-[4,5-dimethylthiazol-2-yl]-2,5-diphenyltetrazolium bromide) were supplied by Sigma-Aldrich (St. Louis, MO). A dialysis bag (molecular weight cutoff, 12,000) was purchased from HiMedia (Mumbai, India). High-performance liquid chromatography (HPLC)-grade acetonitrile was supplied by SD Fine Chem Ltd. (Mumbai, India). All other chemicals and solvents were of analytical grade and were procured from local suppliers unless mentioned otherwise. Ultra-high-purity water, produced by a three-stage Milli-Q Plus 185 purification system (Millipore, Bedford, MA), was utilized throughout all experiments.

Parasites. The WHO reference strain of *L. donovani* (MHOM/IN/80/DD8) was used for both *in vitro* and *in vivo* experiments. These parasites and the macrophage cell line J774A were maintained in RPMI 1640 medium (Sigma) supplemented with 10% heat-inactivated fetal bovine serum (HIFBS), 100 U/ml penicillin, and 100 μg/ml streptomycin at 37°C under a humidified 5% (vol/vol) CO_2–air atmosphere (22).

Animals. Male Syrian golden hamsters (*Mesocricetus auratus*) weighing 45 to 50 g, reared in Central Drug Research Institute (CDRI) facilities, were used to study the antileishmanial effects of the AmB nanocarriers. The hamster is the most appropriate experimental model, because it largely reflects the clinical and immunopathological features of progressive human VL, including a relentless increase in visceral parasite burden, cachexia, hepatosplenomegaly, pancytopenia, hypergammaglobulinemia, and ultimately death (23, 24). *In vivo* studies were carried out with the prior approval of the Animal Ethics Committee of the Central Drug Research Institute and according to the guidelines of the Council for the Purpose of Control and Supervision of Experiments on Animals (CPCSEA), Ministry of Social Justice and Empowerment, Government of India.

Fabrication of the CNC from the nanoemulsion template. The polymeric chitosan nanocapsule (CNC) was generated with a preformed chitosan polymer in two steps. First, an oil-in-water (o/w) nanoemulsion template (NET) was formulated by modified spontaneous emulsification-solvent evaporation (25). A probe sonicator (Sonics & Materials, Newtown, CT) was used to supply high energy to prepare the formulation; however, prior to sonication, the oil phase and the water phase were prepared separately. Briefly, the organic phase, consisting of absolute ethanol, 10% (wt/wt) soya bean oil, and 3% (wt/wt) soya lecithin (SL), a nonionic lipophilic emulsifier, was dispersed by means of a magnetic stirrer until the SL had completely dissolved. The aqueous phase, composed of 4% (wt/wt) Tween 80 (a hydrophilic emulsifier), 2.25% (wt/wt) glycerol (an osmotic agent), and water, was obtained by dissolving the stabilizer in the water. Finally, an AmB solution in acidic methanol was added in the oil phase. The NET was produced by adding the oil phase to the aqueous phase, both of which had been adjusted to the same temperature. Afterwards, high energy was supplied by a sonifier at 40% amplitude for 4 min, and the excess of the solvent mixture (ethanol-water) was subsequently removed under reduced pressure at 50°C until the desired final volume (10 ml) was reached.

Second, the CNC nanocarrier was generated by coating droplets of the NET with the chitosan deposition on the water-oil surface (26). In order to prepare CNC-AmB, the chitosan solution using 1% (vol/vol) glacial acetic acid with varying compositions (0.1, 0.2, 0.4, 0.6, 0.8 and 1% [wt/vol] chitosan [designated NC-1, NC-2, NC-4, NC-6, NC-8, and NC-10, respectively]) and ethanol in an equimolar ratio were gradually added in the continuous aqueous phase of the NET at a 1:10 ratio, and the mixture was stirred uncovered at room temperature in order to evaporate the ethanol completely (IKA, Germany). The polymer precipitated onto the droplets, forming chitosan-coated oil nanodroplets (CNC). This CNC dispersion was sterilized by filtration through a disposable syringe filter (0.45 μm; Millipore); no more than 5 ml of the dispersion was filtered through each disposable syringe filter. The CNCs were recovered by ultracentrifugation at 50,000 × *g* for 20 min at 4°C (Beckman Coulter, Fullerton, CA), and the sediment was then lyophilized. To examine *in vitro* cellular internalization, fluorescent fluorescein isothiocyanate (FITC)-loaded nanocarriers were prepared in the same way, incorporating 0.5 mg/ml FITC instead of AmB.

Physicochemical characterization. The average hydrodynamic diameter (D_H) and polydispersity index (PDI) of prepared nanocarriers were determined using photon correlation spectroscopy (PCS), and the zeta potential was determined by electrophoretic mobility with a laser-based multiple-angle particle electrophoresis analyzer at 25°C (Zetasizer Nano ZS; Malvern Instruments, Malvern, Worcestershire, United Kingdom) just after dispersion in deionized water. All of the measurements were performed in triplicate.

Morphological characteristics were ascertained using high-resolution transmission electron microscopy (HR-TEM). For the HR-TEM measurements, samples (1 mg/20 ml) were prepared as a thin aqueous film supported on a 300-mesh copper grid. Negative staining was performed using a droplet of 2% (wt/vol) phosphotungstic acid. Dried samples were directly imaged at an acceleration voltage of 200 kV by using HR-TEM (Tecnai G^2 F20 microscope; FEI, Eindhoven, The Netherlands).

In order to quantify the amount of AmB loaded into the nanocarrier, a certain amount of the formulation was dispersed in dimethyl sulfoxide in triplicate, vortexed for 20 min, and centrifuged for 20 min at 2,767 × *g*. Afterwards, 1 part of the supernatant was mixed with 9 parts of methanol, and the AmB in the resulting solution was quantified by high-performance liquid chromatography (LC-10ATvp HPLC instrument; Shimadzu, Tokyo, Japan) using a LiChrospher reverse-phase C_{18} column (250 by 4 mm; particle size, 5 μm; Merck, Darmstadt, Germany) with acetonitrile–potassium dihydrogen phosphate buffer (pH 3.5; adjusted with orthophosphoric acid) (60:40, vol/vol) as the mobile phase at a flow rate of 1.0 ml/min. The column effluent was detected with a UV detector at 405 nm. Results are expressed as actual AmB loading (DL) (mg of AmB encapsulated per 100 mg of formulation) and encapsulation efficiency (EE) (ratio of actual to theoretical AmB loading × 100) and are means ± standard deviations (SD) for five different batches.

A dialysis membrane diffusion technique was utilized to investigate the profile of release of AmB from the nanocarriers (27). The dialysis bags were filled with samples of the formulation at a volume equivalent to 2 mg of AmB, hermetically sealed, and suspended in a dissolution apparatus

(model Disso 2000; Labindia, India) containing 250 ml of phosphate-buffered saline (PBS) (pH 7.4) along with 0.5% Tween 80, thermostated at 37 ± 1°C with moderate shaking at 100 rpm. At predetermined time intervals, aliquots of the external release medium (1 ml) were withdrawn, replenished with an equal volume of fresh PBS, and analyzed for the amount of AmB released by using the HPLC method as described above.

The nanocarriers were incubated with 10% (by weight) bovine serum albumin (BSA) solution or 0.2 M $CaCl_2$ solution at room temperature at a concentration of 1 mg/ml. At each time point, an aliquot of the sample solution was collected to measure the size using PCS as described above.

***In vitro* biological evaluation. (i) Macrophage uptake study.** A qualitative *in vitro* uptake experiment was performed in order to examine the effect of the surface modification of the NET with chitosan on the endocytic internalization mechanism that was responsible for enhanced internalization of the CNC. Noninfected J774A cells (10^5/well) were seeded into 96-well plates and were incubated with the NET and chitosan-coated NET (i.e., CNC) formulations incorporating FITC as the fluorescent marker (0.1 mol%) for 24 h. Cell-associated fluorescence was analyzed using a fluorescence-activated cell sorter (FACS) (FC 500 MPL; Beckman Coulter) at an excitation wavelength of 485 nm and an emission wavelength of 538 nm.

(ii) Toxicity determination assay. *(a) In vitro* cytotoxicity for noninfected J774A MPϕ. The cytotoxicity of AmB-loaded formulations was assessed by the MTT proliferation assay (28). Noninfected J774A macrophages (5×10^4/well) were aliquoted into 96-well plates and were incubated in triplicate with either NET-AmB, CNC-AmB, or commercial Fungizone (AmB formulated in 41 mg sodium desoxycholate with 20.2 mg sodium phosphate buffer) or AmBisome (AmB formulated with 213 mg hydrogenated soya phosphatidylcholine, 52 mg cholesterol, 84 mg distearoyl phosphatidylglycerol, 0.64 mg alpha tocopherol, 900 mg sucrose, and 27 mg disodium succinate hexahydrate as the buffer to form a liposome) at equivalent AmB concentrations of 0.25, 2.5, 12.5, and 25 μg/ml at 37 ± 1°C for 24 h. At a determined time, the formulations were replaced with Dulbecco's modified Eagle medium (DMEM) containing MTT (500 μg/ml), and cells were then incubated for an additional 4 h, facilitating the reduction of MTT by viable cells with the formation of purple formazan crystals. MTT was aspirated off, and dimethyl sulfoxide (200 μl) was added to ensure the solubilization of the formazan crystals. Optical density (OD) at 570 nm was measured using a multiwell microplate reader (PowerWave XS; BioTek). The experiment was repeated for reproducibility, and the AmB concentration required to kill 50% of the cells (50% cytotoxic concentration [CC_{50}]) was calculated using sigmoidal regression analysis by plotting a graph of the ODs against the AmB concentration and taking the OD of the control well as 100% viability.

***(b) In vitro* erythrocyte toxicity.** The erythrocyte toxicity assay was performed by following a previously reported procedure with minor modifications (29) to assess the hemolytic potential of the injectable nanocarriers. Erythrocytes were collected by centrifugation (1,420 × *g* for 5 min) from the blood of Wistar rats and were resuspended in PBS. The erythrocyte suspension in PBS served as the negative control, and the erythrocyte suspension that was dispersed in deionized water, considered to be producing 100% hemolysis, provided the positive control. For the study of hemolysis, the erythrocyte suspension was incubated in triplicate with NET-AmB, CNC-AmB, or commercial Fungizone or AmBisome at equivalent AmB concentrations of 0.25, 2.5, 12.5, and 25 μg/ml at 37 ± 1°C for 30 min. After centrifugation at 9,300 × *g* for 20 min, the hemoglobin released into the supernatant was analyzed by measuring the absorbance at 576 nm using a multiwell microplate reader.

(iii) *In vitro* inhibitory effect on intra-MPϕ *L. donovani* amastigotes. The activities of NET-AmB and CNC-AmB against intracellular amastigotes were evaluated according to a protocol described previously (30). Briefly, MPϕ (10^5/well) in 24-well plates (Nunc, IL) were infected with promastigotes expressing green fluorescent protein (GFP) at a multiplicity of 10 parasites per MPϕ. After 12 h of incubation, 24-well plates were washed three times with PBS (pH 7.2) to remove nonphagocytosed promastigotes and were resupplemented with complete RPMI 1640 medium (Sigma). The cells were incubated with AmB-loaded NET-AmB, CNC-AmB, or commercial Fungizone or AmBisome at different drug concentrations, or with drug-free NET or CNC with the same amount of the formulation, in triplicate for 48 h. The untreated infected MPϕ served as a control. After 48 h of treatment, cells were removed, washed in PBS, and quantitated by flow cytometry in a system equipped with a 20-mW argon laser with excitation at 488 nm and emission at 515 nm. Multiparametric data were analyzed by Kaluza analysis software (Becton Dickinson). The inhibition of parasite growth was determined by comparing the fluorescence levels of drug-treated parasites with those of untreated control parasites. The 50% inhibitory concentration (IC_{50}) of each compound was calculated by linear regression analysis.

***In vivo* biological evaluation. (i) *In vivo* AmB assay with *L. donovani*-infected hamsters.** The effects of NET-AmB, CNC–AmB, Fungizone, and AmBisome at doses equivalent to 1 mg of drug/kg of body weight on *in vivo* efficacy against *L. donovani* amastigotes were studied in a hamster model (31). After 30 days of established infection, hamsters (5 per group) were dosed by the intraperitoneal route for 5 consecutive days with AmB-loaded formulations at 1 mg/kg. A group of untreated infected hamsters was used as a control. Treated-hamster groups were sacrificed 1 week after treatment and were compared with the untreated infected control group. The spleen dab smears of all animals were monitored microscopically by using Giemsa-stained imprints in which parasite burdens were measured by counting the number of amastigotes per 100 MPϕ nuclei. The percentage of inhibition (PI) was calculated as (PP − PT/PP) × 100, where PP is the number of amastigotes per 100 MPϕ nuclei in the spleen before treatment and PT is the number of amastigotes per 100 MPϕ nuclei after treatment (32).

(ii) *In vivo* immunomodulatory responses in *L. donovani*-infected hamsters. Quantitative real-time PCR (qRT-PCR) was performed in triplicate to assess the expression of mRNAs for various cytokines (TNF-α, IL-12, IL-4, IL-10, and transforming growth factor β [TGF-β]) and inducible NO synthase (iNOS) in splenic cell smears of differently treated infected hamsters as recommended by the manufacturer. mRNA from splenocytes of different groups of experimental hamsters was isolated using Tri reagent (Sigma) according to the manufacturer's protocol. cDNA was synthesized using a first-strand cDNA synthesis kit (Fermentas) according to the manufacturer's protocol. qRT-PCR was conducted under the following conditions: initial denaturation at 95°C for 2 min, followed by 40 cycles, each consisting of denaturation at 95°C for 30s, annealing at 55°C for 40 s, and extension at 72°C for 40 s, using the iQ5 multicolor real-time PCR system (Bio-Rad). cDNAs from infected hamsters were used as comparator samples. The PCR signals were quantified by comparing the cycle threshold (C_T) value of the gene of interest with the C_T value of the reference gene, encoding hypoxanthine phosphoribosyltransferase (HPRT). Values are expressed as the fold increase (fold change [FC]) in the level of mRNA relative to that in unstimulated cells.

Statistical analysis. Values are presented as means ± SD of three to five independent measurements. The statistical significance of differences was analyzed by one-way analysis of variance (ANOVA), and *P* values less than 0.05 were considered to be statistically significant.

RESULTS

Fabrication and characterization of nanocapsules. CNCs were produced by applying a polymer deposition and adsorption approach, where chitosan was allowed to become electrostatically anchored to, and deposited onto, a negatively charged water-oil

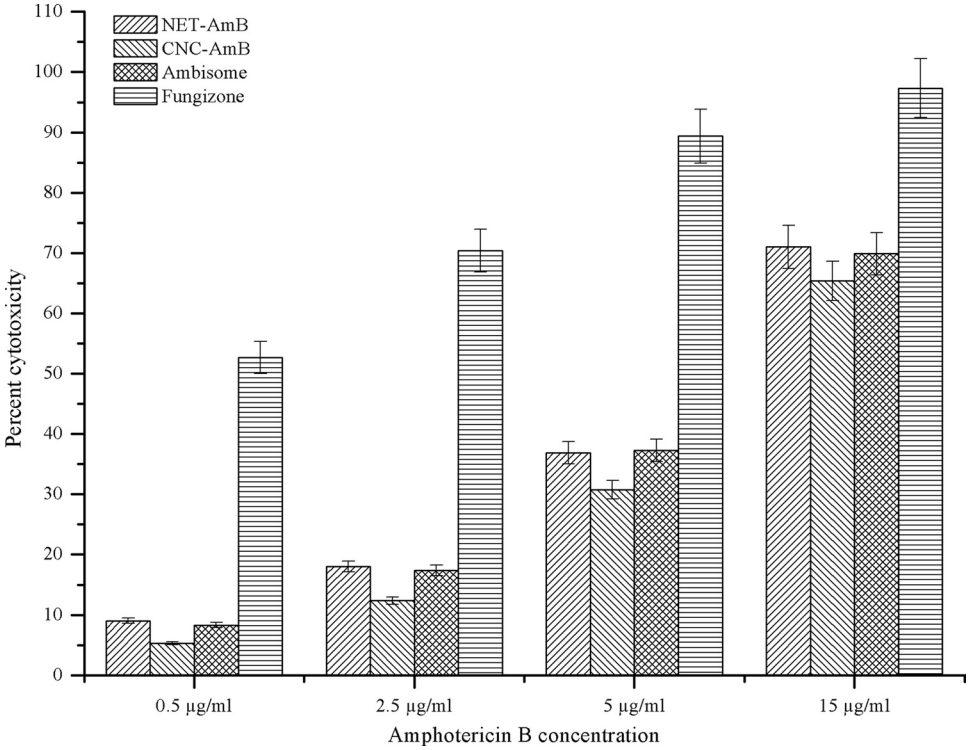

FIG 1 Mitochondrial toxicities (MTT test) of AmB-loaded formulations (NET-AmB and CNC-AmB) and comparison with those of the commercial formulations Fungizone and AmBisome against J774A macrophages after 24 h of incubation at 37°C (under 5% CO_2). A total of 1×10^5 cells/well were incubated in RPMI medium supplemented with 5% HIFBS.

surface of NET droplets produced by the application of ultrasound energy using sonifiers, with Tween 80 and SL as surfactants and with soya bean oil as the central oily core. The excipients that we have used in the formulation are generally considered safe for use in parenteral formulations. The combination of surfactants with oils to form the NET offers an advantage over commercial micellar or cosolvent systems in terms of drug solubilization capacities for amphiphilic compounds (33). The chitosan concentration was optimized by measuring the change in zeta potential, size, and stability of nanocapsule dispersions. The CNC prepared using 0.6% (wt/vol) chitosan (NC-6) had an electric charge of $+29 \pm 0.82$ mV and a size of 145.8 ± 8.91 nm ($n = 3$) and was observed to be the most stable formulation. NC-4 (0.4% [wt/vol] chitosan) showed aggregation characteristics, while NC-8 exhibited a larger size (see Fig. S2 in the supplemental material). Therefore, the 0.6% (wt/vol) chitosan concentration was selected for optimized CNCs. The characteristics of the optimized formulations (the NET and CNC of NC-6) are shown in Table S1 in the supplemental material. The mean sizes (PDI) of the NET and CNCs were ca. 101.4 ± 7.08 nm (0.105 ± 0.03) and 145.8 ± 8.91 nm (0.122 ± 0.04), respectively ($n = 3$), as determined by PCS. HR-TEM explorations of the optimized delivery system confirmed the nanometric sizes of the carriers (100 to 150 nm). The relevant results from the TEM study (see Fig. S3 in the supplemental material) illustrate that the prepared CNC has a spherical morphology, and the development of the CNC is revealed by the continuous chitosan shielding layer, about 16 nm thick, over plain NET droplets. The formulations we developed were found to be highly efficient at AmB entrapment (see Table S1 in the supplemental material). Fig. S4 in the supplemental material shows the cumulative percentages of AmB released as a function of time. These curves showed greater release of AmB from the NET than from CNCs in the initial 24-h period, after which the level of drug release from swelled CNCs increased. The results of the stability study (see Fig. S5 in the supplemental material) demonstrated higher stability of CNC-AmB than of NET-AmB and the commercial formulations.

Assessment of AmB formulation toxicities. (i) Cytotoxicity for J774A MPϕ. The metabolism of treated cells was measured by the reduction of MTT by mitochondria. The cytotoxicity induced by various concentrations of AmB formulations is shown in Fig. 1. The rank order of cytotoxicity of the four formulations against the J774A cell line, from the lowest to the highest CC_{50}, was as follows: Fungizone (CC_{50}, 0.41 ± 0.05 μg/ml), NET-AmB (9.61 ± 0.16 μg/ml), AmBisome (9.84 ± 0.16 μg/ml), CNC-AmB (10.96 ± 0.11 μg/ml). The results demonstrated that the CNC-AmB formulation is considerably less cytotoxic than Fungizone but only slightly less cytotoxic than AmBisome (higher CC_{50}).

(ii) Hemotoxicity for erythrocytes. Formulated CNC-AmB exhibited levels of hemotoxicity as high as $3.291\% \pm 0.82\%$, and NET-AmB showed levels as high as $7.832\% \pm 1.675\%$, whereas the commercial formulations AmBisome and Fungizone showed hemotoxicity levels as high as $5.321\% \pm 1.02\%$ and 100%, respectively (Table 1). All formulations tested had AmB concentrations in the range of 0.25 to 25 μg/ml.

***In vitro* uptake studies.** Figure S6 in the supplemental material depicts the uptake of nanocarrier formulations by J774A macrophages, as determined by flow cytometry analysis. This study rep-

TABLE 1 Hemolytic potentials of various AmB-loaded nanocarriers and commercial formulations at different drug concentrations

Concn (μg/ml)	% Hemolysis[a]			
	NET-AmB	CNC-AmB	AmBisome	Fungizone
0.25	0.167 ± 0.34	0.029 ± 0.21	0.087 ± 0.18	0.973 ± 0.72
5	0.639 ± 0.24	0.552 ± 0.41	0.537 ± 0.19	1.986 ± 0.84
10	2.439 ± 0.54	1.973 ± 0.94	2.313 ± 0.89	10.816 ± 1.02
25	7.832 ± 1.67	3.291 ± 0.82	5.321 ± 1.02	100

[a] Data are reported as means for 3 independent experiments ± SD.

resents comparative uptake of the NET and CNC. Here we revealed that the uptake of CNCs by J774A cells was almost two times (>1.87) enhanced over the uptake of NET.

Assessment of the antileishmanial efficacy of the AmB formulation. (i) *In vitro* assessment for intra-MPϕ *L. donovani* amastigotes. The concentrations of AmB at which 50% and 90% of clinical isolates of *L. donovani* amastigotes were killed (IC_{50} and IC_{90}, respectively) were calculated by flow cytometry using log-phase transgenic GFP-expressing intracellular amastigotes. The percentage of cell death was measured in terms of the decrease in mean fluorescence intensity (MFI) values upon treatment with different concentrations of the formulations. The results are presented as dose-response curves (Fig. 2) and also as IC_{50}s and IC_{90}s (Fig. 3). It was observed that the IC_{50}s of CNC-AmB and NET-AmB were 0.19 ± 0.04 and 0.31 ± 0.05 μg/ml, while those of AmBisome and Fungizone were 0.29 ± 0.03 and 0.48 ± 0.05 μg/ml, respectively. It is evident that the activity of the CNC-AmB formulation is 1.5 times, 1.4 times, and 2.4 times higher than those of NET-AmB, AmBisome, and Fungizone, respectively (P, <0.05 for all three comparisons).

(ii) *In vivo* assessment of antileishmanial efficacy in *L. donovani*-infected hamsters. The results of an *in vivo* experiment (Table 2) clearly manifested that CNC-AmB was significantly more active (86.1% ± 2.08% inhibition) than NET-AmB (64.4% ± 6.91% inhibition), whereas 69.8% ± 3.13% and 55.5% ± 4.34% parasite inhibition was observed with AmBisome and Fungizone, respectively. The rank order of antileishmanial efficacy for the four formulations, from highest to lowest, was as follows: CNC-AmB, AmBisome, NET-AmB, Fungizone.

Quantitative RT-PCR studies of mRNA expression by *L. donovani*-infected hamsters. The antileishmanial efficacy of CNC-AmB was supported by a surge in iNOS, TNF-α, and IL-12 mRNA levels. The mRNA levels of the Th-2 cytokines IL-4, IL-10, and TGF-β, on the other hand, were observed to be downregulated in treated hamsters. This study showed significant differences between the treated and control groups (Fig. 4).

DISCUSSION

A variety of intracellular parasites, including *Leishmania*, can survive and multiply within cells of the mononuclear phagocytic system, particularly MPϕ, which serve as a reservoir for the parasites owing to their ability to resist phagocytosis. Nanocarrier systems can be advantageous in treating these types of infection, because the drug-bearing nanocarriers are concentrated within phagocytes and make direct contact with the parasites.

In the present study, we developed and evaluated a novel, stable nanoemulsion template (NET)-based lipid formulation, CNC-AmB, for the treatment of *L. donovani* infection *in vitro* and

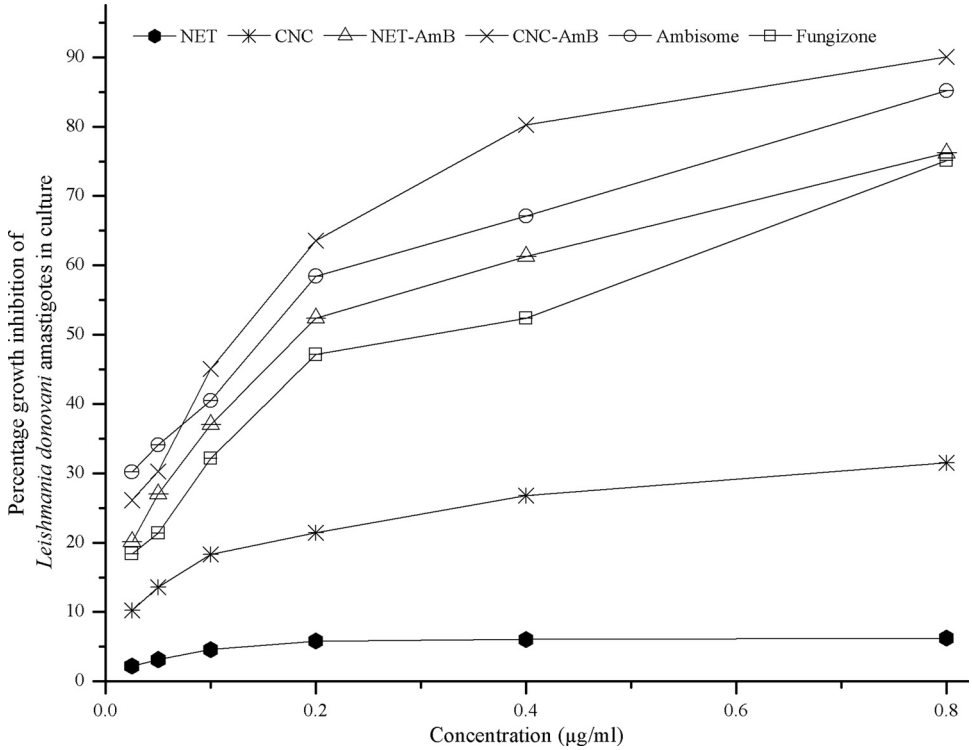

FIG 2 *In vitro* dose-response curves of AmB-loaded NET-AmB and CNC-AmB, Fungizone, AmBisome, and AmB-free NET and CNC against macrophages infected with *L. donovani* amastigotes and observed after 48 h of incubation. All formulations tested were used in the same amounts.

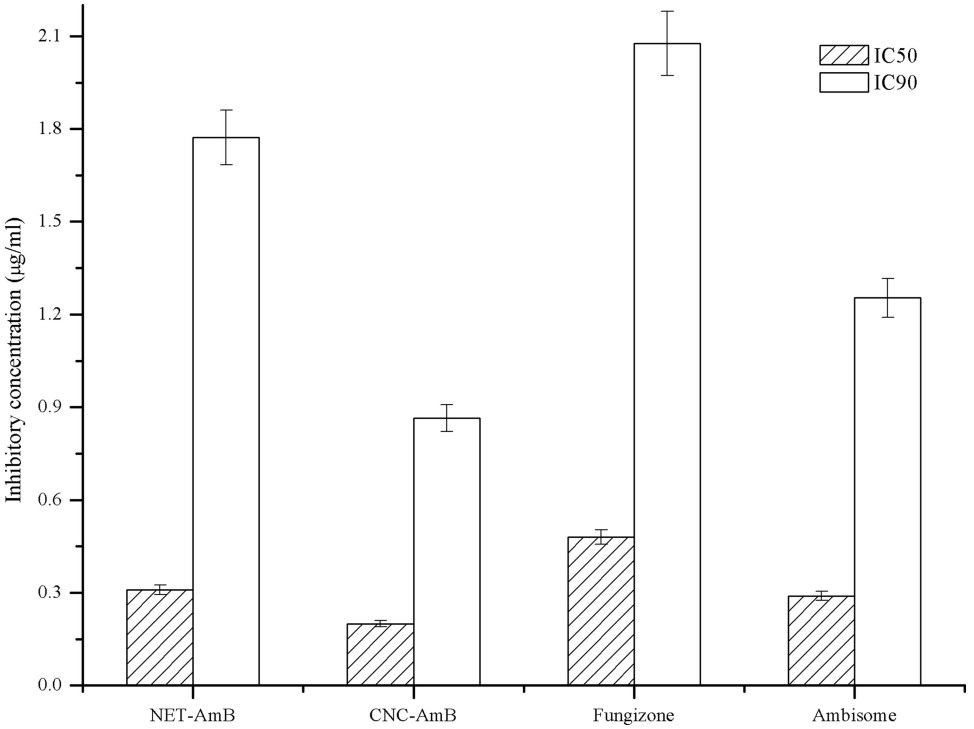

FIG 3 *In vitro* antileishmanial activities (IC_{50} and IC_{90}) of NET-AmB and CNC-AmB compared to those of Fungizone and AmBisome in macrophages infected with *L. donovani* amastigotes, observed after 48 h of incubation.

in vivo, and we assessed its toxicity profile. Additionally, we investigated the changes in the phagocytosis activity of MPϕ and in their production of cytokines after stimulation by CNC-AmB. To assess the efficacy of CNC-AmB, we compared it with NET-AmB and the commercial formulations Fungizone and AmBisome.

Biocompatible excipients were chosen for the primary NET formulation, mainly soybean oil as a hydrophobe to generate the core/shell of the CNC and, in the aqueous phase, the nonionic surfactant Tween 80 and Milli-Q water. An additional, somewhat neutral component, SL, which increases the nanoemulsion stability significantly, creating a "framework" in the shell (34–36), was introduced into the formulation. Indeed, the addition of surfactants has been shown to be an important parameter that efficiently reduces the size of droplets (37). The combination of surfactants with oils to form the NET offers an advantage over a micellar or cosolvent system in terms of drug solubilization capacities for lipophilic compounds, because of the extra locus for solubilization provided by the oil phase (33). The chitosan polymer was added in the continuous phase (even after nanoemulsion was complete), and its deposition onto the emulsion droplets was induced by solvent evaporation, resulting in the formation of the CNC shell.

TABLE 2 *In vivo* antileishmanial activities of NET-AmB and CNC-AmB compared to those of Fungizone and AmBisome in the established model of Syrian golden hamsters infected with *L. donovani* amastigotes[a]

Treatment group ($n = 5$) or condition	No. of amastigotes/100 MPϕ nuclei[b]	% Inhibition of splenic amastigotes[c]
Before treatment	402.2 ± 42.31	
NET-AmB	143.3 ± 25.42	64.4 ± 6.91
CNC-AmB	55.8 ± 10.31	86.1 ± 2.08
Fungizone	178.9 ± 28.44	55.5 ± 4.34
AmBisome	121.6 ± 4.83	69.8 ± 3.13

[a] A shortened treatment course was given, consisting of 5 intraperitoneal injections over a 5-day period (on days 31, 32, 33, 34, and 35 postinfection), making a total dose of 5 mg of AmB/kg of hamster body weight.
[b] The NET-AmB group is statistically significantly different from the Fungizone and AmBisome groups ($P < 0.01$), and the CNC-AmB group is statistically significantly different from the Fungizone and AmBisome groups ($P < 0.05$), by the Tukey test followed by Dunn's multiple-comparison test.
[c] The NET-AmB group is statistically significantly different from the Fungizone and AmBisome groups ($P < 0.01$), and the CNC-AmB group is statistically significantly different from the Fungizone and AmBisome groups ($P < 0.01$), by the Tukey test followed by Dunn's multiple-comparison test.

The zeta potential value and nanometric size are important particle characteristics that can influence both nanocarrier stability and cell adhesion (38). The high positive zeta potential of the CNC, due to the continuous opaque shielding layer (thickness, ca. 15.4 nm) of chitosan, and its particulate form (150 to 200 nm), as confirmed by the HR-TEM study, provide stability to the formulation. Moreover, CNCs are preferentially engulfed by MPϕ due to the easy interaction of cationic particles with negatively charged surfaces of MPϕ by ionic adsorption, promoting subsequent cellular uptake leading to passively targeted drug delivery (39).

The AmB molecule was entrapped (efficiency, 97.8% ± 2.11%) in the CNC formulation by intercalation between the hydrophilic chitosan polymer and hydrophobic cavitation bubbles, i.e., the oil core, generated by a succession of mechanical depressions and compressions in the liquid dispersion of the NET due to sonifier energy (40). The minor decrease in the entrapment efficiency of CNCs relative to that of the NET may be partially due to longer exposure of NET droplets to the solvent during the modification process, leading to a loss of the drug (see Table S1 in the supplemental material). Figure S4 in the supplemental material

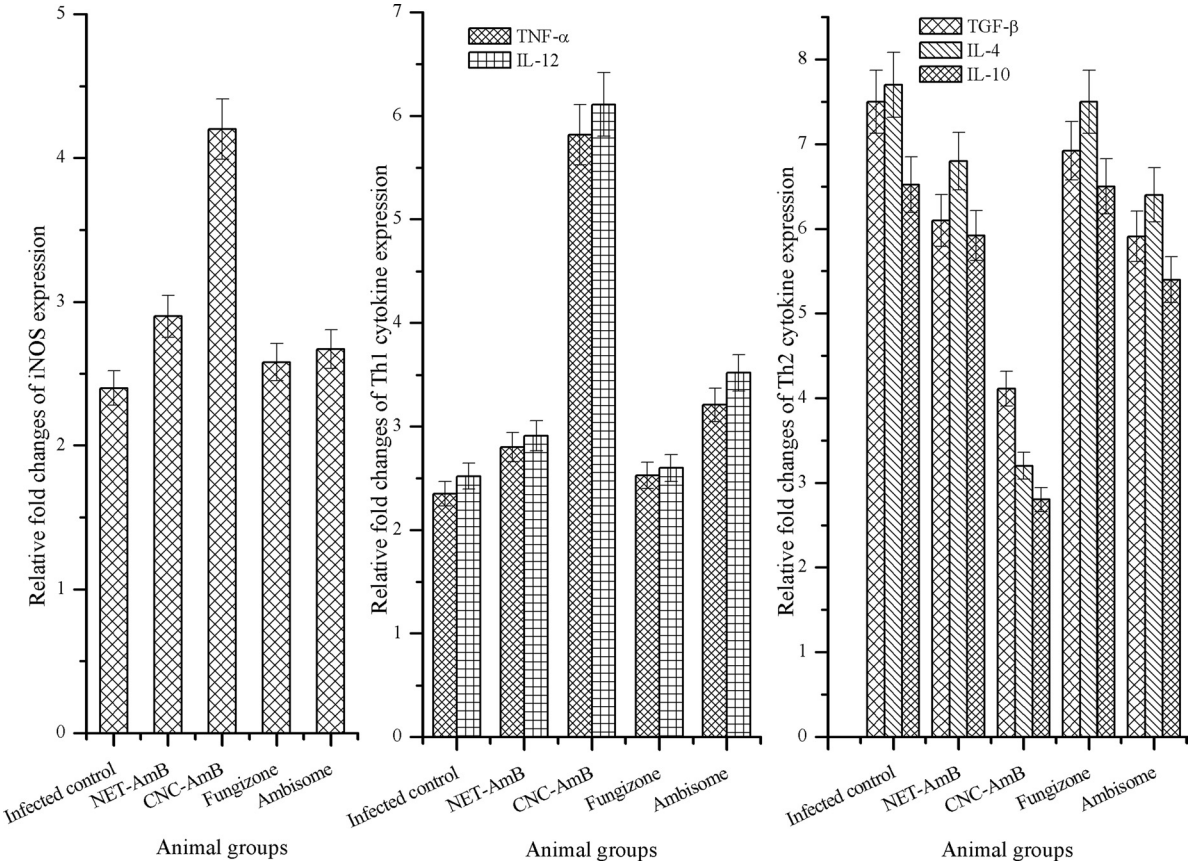

FIG 4 *In vivo* immunomodulatory responses. Splenic iNOS and cytokine (TNF-α, IL-12, IL-4, IL-10, and TGF-β) mRNA expression in infected control and treated (NET-AmB, CNC-AmB, Fungizone, or AmBisome) Syrian golden hamsters was determined by quantitative RT-PCR. Bar graphs show the mean fold changes in iNOs and cytokine expression levels ± SD (5 hamsters/time point) relative to the level of expression of the reference gene (encoding HPRT).

shows that the release ratio of the drug from NET-AmB significantly exceeded that with CNC-AmB in 24 h, indicating restriction of drug release due to the chitosan surface layer. Thereafter, release from CNC-AmB increased comparatively because of the hydrophilic chitosan, which allows greater ease of penetration of the release medium, facilitating the release of AmB from the swelled CNCs. However, it has been reported that the incorporation of AmB into fat emulsions resulted in the precipitation of AmB (41), whereas in the CNCs, AmB is highly stable.

Because nanocarrier stability is greatly influenced by the surface charge (zeta potential), as shown in Fig. S5 in the supplemental material, negatively charged NET droplets (the negative charge is attributed mainly to the presence of the natural surfactant lecithin) exhibited a higher increase in size, due to lower stability, than did positively charged CNCs. The negative charge of the NET forces the adsorption of cationic proteins and sodium and calcium ions that are present in the biological fluids (serum), leading to the neutralization of the surface charge, the breakdown of the system, and the leakage of the entrapped agents. On the other hand, positively charged chitosan-surfactant layers around NET droplets in the CNC carrier provided long-term stability.

The model drug AmB and its commercial formulations are well known for hemotoxicity, due to eryptosis triggered by cell membrane scrambling and cell shrinkage through the stimulation of increased Ca^{2+} entry into erythrocytes (42). AmB-induced hemolysis was studied *in vitro*, providing a reliable measure for estimating the membrane damage caused *in vivo*. Evaluation of the toxicity measurements of CNC-AmB against the J774A cell line clearly demonstrated its comparative nontoxicity (CC_{50}, 10.96 μg/ml, higher than those of commercial formulations) for MPϕ, due to the hemocompatibility behavior of chitosan (43).

When evaluated by *in vitro* MPϕ uptake studies, CNC-AmB showed greater levels of internalization than NET-AmB (see Fig. S6 in the supplemental material). It has been shown that expression of activation markers, such as major histocompatibility complex (MHC) classes I and II, Fc receptors, and the mannose receptor, is induced after chitosan treatment (18, 44). It is possible that the binding of the *N*-acetylglucosamine unit of the low-molecular-weight chitosan of CNCs favors recognition by these receptors, which mediate the internalization of the drug carrier, which, in turn, is thought to be a prerequisite for enhancing the activation of inflammatory cells, including MPϕ, the favored site of *L. donovani* replication (14, 45). Increased delivery of CNCs to the MPϕ population would be expected to result in increased efficacy of CNC-AmB in *Leishmania*-infected MPϕ and hamsters.

When evaluated by *in vitro* studies, AmB in the novel formulations retained its antileishmanial activity against intra-MPϕ amastigotes. The 50% parasite growth-inhibitory effectiveness of the CNC-AmB formulation for the amastigotes, the stage responsible for VL, was 1.5-fold, 1.4-fold, and 2.4-fold better than those

of NET-AmB, AmBisome, and Fungizone, respectively. These results supported the results of in *vivo studies* with golden hamsters in which the inhibition of *L. donovani* infection was significantly greater with CNC-AmB. The commercial formulation AmBisome, with a liposomal drug carrier, was 1.65 times more efficacious than Fungizone ($P < 0.05$). It is interesting that the NET-AmB formulation is more effective than Fungizone and similar in effectiveness to AmBisome, while CNC-AmB is more effective than AmBisome (Table 2), suggesting that the difference in the activity of CNC-AmB is attributable to uptake and interaction with host cells rather than to intracellular distribution. The results demonstrated that at 1 mg/kg AmB, under the treatment regimen employed, CNC-AmB elicited a marked improvement over AmBisome in terms of parasite burden and survival. The substantially increased efficacy and decreased toxicity are concordant with the findings of previous studies of lipid-complexed AmB formulations (46, 47).

Accumulating evidence has shown that in hamsters, protection against *Leishmania* is associated with Th2-to-Th1 switching for complete parasite clearance. For this reason, we assessed several Th1 (TNF-α, IL-12) and Th2 (TGF-β, IL-4, and IL-10) cytokines to investigate the possible role of the cytokine immune response in drug-free CNC and CNC-AmB treatment of VL. Furthermore, the iNOS chemokine in MPϕ can be induced by many cytokines (48). After activation, MPϕ respond to the particulate CNC-AmB carrier via phagocytosis and secrete proinflammatory cytokines. This may lead to a cascade of adverse reactions, which sometimes cause severe damage to the host. Therefore, the production of proinflammatory cytokines and the internalization response were utilized to evaluate the interaction between the nanocarrier and MPϕ. The results of this study demonstrated that chitosan induced significantly elevated release of the cytokines TNF-α and IL-12 (Fig. 4; see also Fig. S7 in the supplemental material), confirming the reactivity of the J774 cells with splenic MPϕ and consequent Th1-mediated protection (49). The results presented here show that LMW chitosan moderately activated the iNOS pathway in resident MPϕ, as reported previously (50). Additionally, a cumulative effect of IL-12 along with iNOS probably mediated parasite killing (51, 52). Conversely, the results showed favorable decreases in the infection-susceptible expression of the IL-10, IL-4, and TGF-β genes, which are potent inhibitors of MPϕ activation and of the killing of *Leishmania* organisms (53, 54). Decisively, our scientific findings suggest that CNC-AmB treatment may function as well in immunocompromised patients as in immunocompetent patients, thus increasing its potential efficacy in human immunodeficiency virus–leishmaniasis coinfection therapy.

Conclusion. CNC-AmB represents a novel colloidal carrier, remarkably effective for experimental visceral *L. donovani* infection in hamsters. At an equivalent dosage and treatment frequency, it far surpasses commercial AmB formulations and results in effective clearance of parasites by using a limited, biologically safe, and widely spaced therapeutic regimen. The presence of discernible changes in the cytokine responses indicates that this immunochemotherapeutic strategy is dependent on host cytokine-based immunity. CNC-AmB can be considered a "potential protective AmB delivery system." In addition, the composition and manufacturing procedures of CNCs make feasible the production of a stable AmB delivery system that could be an economically interesting alternative to the current high-cost commercial lipid-based formulations. The present work clearly supports the application of nanoemulsion template-based chitosan nanocapsules as a novel therapeutic AmB delivery approach for safer and cost-effective treatment of VL.

ACKNOWLEDGMENTS

This work was supported by a grant from the Department of Biotechnology, Government of India, New Delhi, India (BT/PR2007/MED/29/311/2011). S.A. thankfully acknowledges the Indian Council of Medical Research, New Delhi, India, for awarding a Senior Research Fellowship.

We thank the Electron Microscope Facility at the Department of Anatomy, All India Institute of Medical Sciences (AIIMS, New Delhi, India) for providing HR-TEM analysis. We also thank the Sophisticated Analytical Instrument Facility Division (CDRI, Lucknow, India) for flow cytometry analysis.

REFERENCES

1. **World Health Organization.** 2010. Control of the leishmaniases: report of a meeting of the WHO Expert Committee on the Control of Leishmaniases, Geneva, 22–26 March 2010, p 5–12. Technical report series 949. World Health Organization, Geneva, Switzerland.
2. **Chappuis F, Sundar S, Hailu A, Ghalib H, Rijal S, Peeling RW, Alvar J, Boelaert M.** 2007. Visceral leishmaniasis: what are the needs for diagnosis, treatment and control? Nat. Rev. Microbiol. **5**:873–882.
3. **Malla N, Mahajan RC.** 2006. Pathophysiology of visceral leishmaniasis—some recent concepts. Indian J. Med. Res. **123**:267–274.
4. **Handman E.** 2001. Leishmaniasis: current status of vaccine development. Clin. Microbiol. Rev. **14**:229–243.
5. **World Health Organization.** 2010. Control of the leishmaniases: report of a meeting of the WHO Expert Committee on the Control of Leishmaniases, Geneva, 22–26 March 2010, p 104. Technical report series 949. World Health Organization, Geneva, Switzerland.
6. **Pourshafie M, Morand S, Virion A, Rakotomanga M, Dupuy C, Loiseau PM.** 2004. Cloning of *S*-adenosyl-L-methionine:C-24-Δ-sterol-methyltransferase (ERG6) from *Leishmania donovani* and characterization of mRNAs in wild-type and amphotericin B-resistant promastigotes. Antimicrob. Agents Chemother. **48**:2409–2414.
7. **Dupont B.** 2002. Overview of the lipid formulations of amphotericin B. J. Antimicrob. Chemother. **49**(Suppl. 1):31–36.
8. **Townsend RW, Zutshi A, Bekersky I.** 2001. Biodistribution of 4-[^{14}C]cholesterol-AmBisome following a single intravenous administration to rats. Drug Metab. Dispos. **29**:681–685.
9. **Sánchez-Brunete JA, Dea MA, Rama S, Bolas F, Alunda JM, Torrado-Santiago S, Torrado JJ.** 2004. Amphotericin B molecular organization as an essential factor to improve activity/toxicity ratio in the treatment of visceral leishmaniasis. J. Drug Target. **12**:453–460.
10. **Hiemenz JW, Walsh TJ.** 1996. Lipid formulations of amphotericin B: recent progress and future directions. Clin. Infect. Dis. **22**(Suppl. 2):S133–S144.
11. **Wong-Beringer A, Jacobs RA, Guglielmo BJ.** 1998. Lipid formulations of amphotericin B: clinical efficacy and toxicities. Clin. Infect. Dis. **27**:603–618.
12. **Chandy T, Sharma CP.** 1990. Chitosan—as a biomaterial. Biomater. Artif. Cells Artif. Organs **18**:1–24.
13. **Dornish M, Kaplan DS, Arepalli SR.** 2012. Regulatory status of chitosan and derivatives, p 463–481. *In* Sarmento B, das Neves J (ed), Chitosan-based systems for biopharmaceuticals: delivery, targeting and polymer therapeutics, 1st ed, vol 1.Wiley, Chichester, West Sussex, United Kingdom.
14. **Peluso G, Petillo O, Ranieri M, Santin M, Ambrosio L, Calabro D, Avallone B, Balsamo G.** 1994. Chitosan-mediated stimulation of macrophage function. Biomaterials **15**:1215–1220.
15. **Kushawaha PK, Gupta R, Sundar S, Sahasrabuddhe AA, Dube A.** 2011. Elongation factor-2, a Th1 stimulatory protein of *Leishmania donovani*, generates strong IFN-γ and IL-12 response in cured *Leishmania*-infected patients/hamsters and protects hamsters against *Leishmania* challenge. J. Immunol. **187**:6417–6427.
16. **Seo WG, Pae HO, Kim NY, Oh GS, Park IS, Kim YH, Lee YH, Jun CD, Chung HT.** 2000. Synergistic cooperation between water-soluble chitosan oligomers and interferon-gamma for induction of nitric oxide synthesis and tumoricidal activity in murine peritoneal macrophages. Cancer Lett. **159**:189–195.

17. **Yu Z, Zhao L, Ke H.** 2004. Potential role of nuclear factor-κB in the induction of nitric oxide and tumor necrosis factor-alpha by oligochitosan in macrophages. Int. Immunopharmacol. **4**:193–200.
18. **Shibata Y, Metzger WJ, Myrvik QN.** 1997. Chitin particle-induced cell-mediated immunity is inhibited by soluble mannan: mannose receptor-mediated phagocytosis initiates IL-12 production. J. Immunol. **159**:2462–2467.
19. **Otterlei M, Varum KM, Ryan L, Espevik T.** 1994. Characterization of binding and TNF-α-inducing ability of chitosans on monocytes: the involvement of CD14. Vaccine **12**:825–832.
20. **Feng J, Zhao L, Yu Q.** 2004. Receptor-mediated stimulatory effect of oligochitosan in macrophages. Biochem. Biophys. Res. Commun. **317**: 414–420.
21. **Ogawa S, Decker EA, McClements DJ.** 2003. Production and characterization of O/W emulsions containing cationic droplets stabilized by lecithin-chitosan membranes. J. Agric. Food Chem. **51**:2806–2812.
22. **Dube A, Singh N, Sundar S.** 2005. Refractoriness to the treatment of sodium stibogluconate in Indian kala-azar field isolates persist in in vitro and in vivo experimental models. Parasitol. Res. **96**:216–223.
23. **Kaur J, Sundar S, Singh N.** 2010. Molecular docking, structure-activity relationship and biological evaluation of the anticancer drug monastrol as a pteridine reductase inhibitor in a clinical isolate of *Leishmania donovani*. J. Antimicrob. Chemother. **65**:1742–1748.
24. **Garg R, Gupta SK, Tripathi P, Hajela K, Sundar S, Naik S, Dube A.** 2006. *Leishmania donovani*: identification of stimulatory soluble antigenic proteins using cured human and hamster lymphocytes for their prophylactic potential against visceral leishmaniasis. Vaccine **24**:2900–2909.
25. **Martini E, Fattal E, de Oliveira MC, Teixeira H.** 2008. Effect of cationic lipid composition on properties of oligonucleotide/emulsion complexes: physico-chemical and release studies. Int. J. Pharm. **352**:280–286.
26. **Paiphansiri U, Tangboriboonrat P, Landfester K.** 2006. Polymeric nanocapsules containing an antiseptic agent obtained by controlled nanoprecipitation onto water-in-oil miniemulsion droplets. Macromol. Biosci. **6**:33–40.
27. **Chourasia MK, Kang L, Chan SY.** 2011. Nanosized ethosomes bearing ketoprofen for improved transdermal delivery. Results Pharma Sci. **1**:60–67.
28. **Seymour AA, Sheldon JH, Smith PL, Asaad M, Rogers WL.** 1994. Potentiation of the renal responses to bradykinin by inhibition of neutral endopeptidase 3.4.24.11 and angiotensin-converting enzyme in anesthetized dogs. J. Pharmacol. Exp. Ther. **269**:263–270.
29. **Bock TK, Muller BW.** 1994. A novel assay to determine the hemolytic activity of drugs incorporated in colloidal carrier systems. Pharm. Res. **11**:589–591.
30. **Mookerjee Basu J, Mookerjee A, Banerjee R, Saha M, Singh S, Naskar K, Tripathy G, Sinha PK, Pandey K, Sundar S, Bimal S, Das PK, Choudhuri SK, Roy S.** 2008. Inhibition of ABC transporters abolishes antimony resistance in *Leishmania* infection. Antimicrob. Agents Chemother. **52**:1080–1093.
31. **Gupta S, Dube A, Vyas SP.** 2007. Antileishmanial efficacy of amphotericin B bearing emulsomes against experimental visceral leishmaniasis. J. Drug Target. **15**:437–444.
32. **Manandhar KD, Yadav TP, Prajapati VK, Kumar S, Rai M, Dube A, Srivastava ON, Sundar S.** 2008. Antileishmanial activity of nano-amphotericin B deoxycholate. J. Antimicrob. Chemother. **62**:376–380.
33. **Lawrence MJ, Rees GD.** 2000. Microemulsion-based media as novel drug delivery systems. Adv. Drug Deliv. Rev. **45**:89–121.
34. **Minkov I, Ivanova T, Panaiotov I, Proust J, Saulnier P.** 2005. Reorganization of lipid nanocapsules at air-water interface. Part I. Kinetics of surface film formation. Colloids Surf. B Biointerfaces **45**:14–23.
35. **Minkov I, Ivanova T, Panaiotov I, Proust J, Saulnier P.** 2005. Reorganization of lipid nanocapsules at air-water interface. Part 2. Properties of the formed surface film. Colloids Surf. B Biointerfaces **44**:197–203.
36. **Yilmaz E, Borchert HH.** 2005. Design of a phytosphingosine-containing, positively-charged nanoemulsion as a colloidal carrier system for dermal application of ceramides. Eur. J. Pharm. Biopharm. **60**:91–98.
37. **Behrend O, Ax K, Schubert H.** 2000. Influence of continuous phase viscosity on emulsification by ultrasound. Ultrason. Sonochem. **7**:77–85.
38. **Vandervoort J, Ludwig A.** 2002. Biocompatible stabilizers in the preparation of PLGA nanoparticles: a factorial design study. Int. J. Pharm. **238**: 77–92.
39. **Kunjachan S, Gupta S, Dwivedi AK, Dube A, Chourasia MK.** 2011. Chitosan-based macrophage-mediated drug targeting for the treatment of experimental visceral leishmaniasis. J. Microencapsul. **28**:301–310.
40. **Anton N, Benoit JP, Saulnier P.** 2008. Design and production of nanoparticles formulated from nano-emulsion templates—a review. J. Control. Release **128**:185–199.
41. **Washington C, Lance M, Davis SS.** 1993. Toxicity of amphotericin B emulsion formulations. J. Antimicrob. Chemother. **31**:806–808.
42. **Mahmud H, Mauro D, Qadri SM, Foller M, Lang F.** 2009. Triggering of suicidal erythrocyte death by amphotericin B. Cell. Physiol. Biochem. **24**: 263–270.
43. **Jumaa M, Furkert FH, Muller BW.** 2002. A new lipid emulsion formulation with high antimicrobial efficacy using chitosan. Eur. J. Pharm. Biopharm. **53**:115–123.
44. **Ueno H, Mori T, Fujinaga T.** 2001. Topical formulations and wound healing applications of chitosan. Adv. Drug Deliv. Rev. **52**:105–115.
45. **Mori T, Okumura M, Matsuura M, Ueno K, Tokura S, Okamoto Y, Minami S, Fujinaga T.** 1997. Effects of chitin and its derivatives on the proliferation and cytokine production of fibroblasts in vitro. Biomaterials **18**:947–951.
46. **Gangneux JP, Sulahian A, Garin YJ, Farinotti R, Derouin F.** 1996. Therapy of visceral leishmaniasis due to *Leishmania infantum*: experimental assessment of efficacy of AmBisome. Antimicrob. Agents Chemother. **40**:1214–1218.
47. **Yardley V, Croft SL.** 2000. A comparison of the activities of three amphotericin B lipid formulations against experimental visceral and cutaneous leishmaniasis. Int. J. Antimicrob. Agents **13**:243–248.
48. **Schmidt HH, Warner TD, Nakane M, Forstermann U, Murad F.** 1992. Regulation and subcellular location of nitrogen oxide synthases in RAW264.7 macrophages. Mol. Pharmacol. **41**:615–624.
49. **Samant M, Gupta R, Kumari S, Misra P, Khare P, Kushawaha PK, Sahasrabuddhe AA, Dube A.** 2009. Immunization with the DNA-encoding N-terminal domain of proteophosphoglycan of *Leishmania donovani* generates Th1-type immunoprotective response against experimental visceral leishmaniasis. J. Immunol. **183**:470–479.
50. **Porporatto C, Bianco ID, Riera CM, Correa SG.** 2003. Chitosan induces different L-arginine metabolic pathways in resting and inflammatory macrophages. Biochem. Biophys. Res. Commun. **304**:266–272.
51. **Basu R, Bhaumik S, Basu JM, Naskar K, De T, Roy S.** 2005. Kinetoplastid membrane protein-11 DNA vaccination induces complete protection against both pentavalent antimonial-sensitive and -resistant strains of *Leishmania donovani* that correlates with inducible nitric oxide synthase activity and IL-4 generation: evidence for mixed Th1- and Th2-like responses in visceral leishmaniasis. J. Immunol. **174**:7160–7171.
52. **Gifawesen C, Farrell JP.** 1989. Comparison of T-cell responses in self-limiting versus progressive visceral *Leishmania donovani* infections in golden hamsters. Infect. Immun. **57**:3091–3096.
53. **Kenney RT, Sacks DL, Gam AA, Murray HW, Sundar S.** 1998. Splenic cytokine responses in Indian kala-azar before and after treatment. J. Infect. Dis. **177**:815–818.
54. **Melby PC, Tryon VV, Chandrasekar B, Freeman GL.** 1998. Cloning of Syrian hamster (*Mesocricetus auratus*) cytokine cDNAs and analysis of cytokine mRNA expression in experimental visceral leishmaniasis. Infect. Immun. **66**:2135–2142.